



Published in final edited form as:

Gene Ther. 2007 February ; 14(3): 191–202.

Sustained Phenotypic Correction in a Mouse Model of Hypoalphalipoproteinemia with a Helper-Dependent Adenovirus Vector

Kazuhiro Oka^{1,2,3}, L. Maria Belalcazar¹, Carrie Dieker¹, Elie A. Nour¹, Patricia Nuno-Gonzalez¹, Antoni Paul¹, Shelley Cormier¹, Jae-Kyung Shin¹, Milton Finegold⁴, and Lawrence Chan^{1,2}

¹Department of Molecular and Cellular Biology, Baylor College of Medicine, Houston, Texas 77030, USA

²Department of Medicine, Baylor College of Medicine, Houston, Texas 77030, USA

³Department of Neurology, Baylor College of Medicine, Houston, Texas 77030, USA

⁴Department of Pathology, Baylor College of Medicine, Houston, Texas 77030, USA

Abstract

We examined the efficacy and host response to the adenovirus (Ad)-mediated delivery of human apolipoprotein A-I (APOA1) gene to the liver of APOA1^{-/-} mice. Administration of a first generation vector (FGAd-AI) resulted in a transient appearance of APOA1 in plasma and induced an anti-APOA1 antibody titer while treatment with a helper-dependent vector (HDAd-AI) resulted in sustained APOA1 expression without inducing an antibody titer. With these results, we studied the effects of FGAd vectors on APOA1 expression by HDAd-AI vector. Co-treatment with a FGAd vector inhibited HDAd-AI-mediated APOA1 expression independent of transgene cassettes, but only FGAd-AI induced a humoral response. Furthermore, APOA1 mRNA levels in mice co-treated with FGAd vectors were much lower than those expected from the vector copy number, suggesting that DNA of FGAd vectors interferes with the HDAd-AI vector's APOA1 promoter. A single treatment with an HDAd-AI vector produced a supraphysiological plasma APOA1 level that gradually declined to about half the normal human level over the course of 2 years, associated with a plasma cholesterol level that is persistently higher than that in controls. This investigation provides the proof of principle that liver-directed HDAd gene delivery is effective for the long-term phenotypic correction of monogenic hypoalphalipoproteinemia.

Keywords

helper-dependent adenovirus; gene therapy; apolipoprotein A-I; hypoalphalipoproteinemia; adaptive immunity

Introduction

High-density lipoprotein (HDL) deficiency constitutes the most common lipid abnormality in patients with coronary artery disease.^{1,2} Each mg/dl increase in circulating HDL cholesterol levels is associated with a 3% reduction in cardiovascular risk.³ Apolipoprotein A-I (APOA1) is the main protein component of HDL and, epidemiological studies suggest that it may be a

better marker of cardiovascular protection than HDL cholesterol itself.⁴ In patients with a congenital deficiency of APOA1, a major cause of familial hypoalphalipoproteinemia, the marked deficiency of plasma HDL predisposes these patients to premature atherosclerosis.^{5,6} Population studies suggest that congenital APOA1 deficiency is not a rare condition.⁷ If effective, long-term APOA1 gene therapy would be a definitive treatment of familial hypoalphalipoproteinemia caused by a congenital APOA1 deficiency. Furthermore, it would also be a method for reversing hypoalphalipoproteinemia or low HDL commonly associated with cardiovascular disease and should significantly reduce the risk of atherosclerotic cardiovascular disease in these patients.

Adenoviral vectors (Ads) efficiently transduce a variety of cell types including hepatocytes independent of cellular proliferation. Helper-dependent Ads (HDAds) are devoid of all viral protein genes; they display greatly attenuated toxicity and prolonged transgene expression following liver transduction *in vivo*.^{8,9,10-14} In this investigation we examined the effect of Ad-mediated gene transfer of the human APOA1 gene to the liver of APOA1^{-/-} mice, a mouse model for human familial hypoalphalipoproteinemia, to reverse the low HDL levels. We compared the efficacy of HDAd and first generation Ad (FGAd-AI) expressing human APOA1 gene to reverse the phenotype of mice with a congenital HDL deficiency. Induced APOA1 expressed in this model is a neoantigen and is predicted to elicit adaptive immunity. Interestingly, a significant anti-APOA1 antibody titer was found in mice treated with FGAd-AI but not with HDAd-AI. The appearance of an anti-APOA1 antibody titer was correlated with a fall in plasma APOA1 and cholesterol levels. To further understand the mechanisms by which FGAd-AI but not HDAd-AI induced an anti-APOA1 antibody titer, we studied the effect of co-injecting FGAd or HDAd with HDAd-AI. Co-injection of FGAd-AI inhibited HDAd-mediated APOA1 expression by inducing an anti-APOA1 antibody titer; it also led to a reduced HDAd-AI copy number in the liver. The fall in plasma APOA1 and decrease in hepatic HDAd-AI copy number were related to the co-injection of FGAd *per se* and not related to the transgene in these vectors. Finally, we monitored the effect of a single injection of HDAd-AI on phenotypic correction of APOA1^{-/-} mice and found persistent, near normal plasma levels of human APOA1 and HDL at the end of two years.

Results

Production and characterization of HDAd vector

Taking advantage of the high capacity of HDAd vectors, we cloned an 11-kb human genomic APOA1 DNA into an HDAd (Fig. 1a). The vector was stable during amplification and exhibited no DNA rearrangement (Fig. 1b). It was free of helper virus contamination by Southern blot analysis (Fig. 1c) and by real-time PCR, which has a detection limit of 0.001%.

Effects of adenoviral vector treatment on plasma cholesterol

To achieve phenotypic correction of an APOA1 deficiency in mice, we must express the APOA1 transgene at a high level to produce a normal APOA1 plasma concentration (100-150 mg/dl).¹ Our experience in two other mouse models of dyslipidemias^{10,11} suggests that a dose in the range of $0.5-4.5 \times 10^{12}$ vector particles (VP)/kg may be required to reverse the phenotype.^{10,11,15} We, therefore, treated APOA1^{-/-} mice with escalating doses of HDAd-AI, starting at 5×10^{11} VP/kg (HDAd-AI-L), increasing by a half-log increment to 1.5×10^{12} VP/kg (HDAd-AI-M), and finally using a maximum dose of 4.5×10^{12} VP/kg (HDAd-AI-H). An additional group of mice was treated with FGAd-AI (4.5×10^{12} VP/kg). Plasma APOA1 was barely detectable in mice treated with the lowest dose (n=4) (Fig. 2a). In HDAd-AI-M group, APOA1 was not detectable at day 3 and appeared in the plasma at a readily detectable level of 29 ± 33 mg/dl (mean \pm SD, n=5) at day 7. It gradually increased to a level similar to normal human subjects (100 – 150 mg/dl) 14 days after treatment (120 ± 75 mg/dl), reaching

a plateau of 141 ± 54 mg/dl at day 28 and remained at this level for 70 days. In mice treated with the highest dose (HDAd-AI-H group), the plasma APOA1 level was not detectable at day 3 but increased to 86 ± 109 mg/dl 7 days after treatment and reached the highest level of 212 ± 43 mg/dl at day 28. In contrast, mice treated with FGAd-AI displayed a markedly elevated plasma APOA1 level (226 ± 105 mg/dl) at day 3 and a peak level of 297 ± 157 mg/dl at day 7. However, the supraphysiological plasma hAPOA1 response following FGAd-AI administration was short-lived, as the protein was no longer detectable in plasma at day 28 (Fig. 2a and 2b).

Appearance of APOA1 in plasma after gene transfer was associated with an increase in plasma cholesterol (Fig. 2c). FGAd-AI injection led to marked hypercholesterolemia that was out of proportion to the rise in plasma APOA1; it went up from a baseline of 29 ± 8 mg/dl to 192 ± 91 mg/dl at day 3 and 365 ± 66 mg/dl at day 7, which may reflect hypercholesterolemia secondary to FGAd-associated liver damage.¹⁶ The level rapidly declined on day 14 and was not significantly different from PBS treated mice on day 28. In contrast, HDAd-AI-M and HDAd-AI-H groups did not show any change in plasma cholesterol until day 7, when it started to rise to a plateau at day 28. Mice treated with the lowest dose (HDAd-AI-L group) did not show any significant change in plasma cholesterol following treatment. At day 84, we fractionated plasma collected from HDAd-AI-H or PBS-treated mice by FPLC. By this analysis, we failed to detect any HDL in PBS-treated APOA1^{-/-} mice. HDAd-AI treatment led to the appearance of a prominent HDL cholesterol peak, the basis of the post-treatment total plasma cholesterol elevation (Fig. 2d).

Toxicity after treatment with FGAd-AI or HDAd-AI

We evaluated indices of hepatotoxicity in FGAd-AI- and HDAd-AI-treated APOA1^{-/-} mice. Plasma alanine aminotransferase (ALT) activity increased significantly in FGAd-AI-treated mice at day 7 and 14 (101 ± 16 and 112 ± 15 IU/l, $p < 0.001$ vs. pretreatment levels of 12 ± 8 IU/l, $n=5$), decreasing to 37 ± 16 IU/l at day 28 ($p < 0.05$ vs. pretreatment). In contrast, there was no significant change in ALT activity in the PBS- or HDAd-AI-treated groups (Fig. 3a). The increase in liver enzyme activity was correlated with abnormal liver histopathology (Fig. 3b and Table 1). Liver sections of FGAd-AI-treated mice at 8 days post-injection, displayed severe diffuse necrosis, increased inflammation, mitoses, hepatocellular nuclear pleomorphism, and atypia. Signs of liver injury remained evident 80 days after treatment. In contrast, HDAd-AI treated mice as well as PBS controls showed minimal architectural disturbances and necroinflammation.

Previous studies in mice and baboons using FGAd and clinical experience with the E1-E4-deleted Ad vector suggest that thrombocytopenia is a sensitive indicator of early toxicity.¹⁷⁻²⁰ We performed complete whole blood counts in mice treated with Ad vectors. Platelet counts dropped markedly in mice treated with 4.5×10^{12} VP/kg of FGAd-AI (90%, $p < 0.001$ vs. pretreatment, $n=5$) or 4.5×10^{12} VP/kg of HDAd-AI (77%, $p < 0.001$, $n=5$) 3 days after injection. They were also significantly reduced, but to a much lesser extent, in mice treated with an intermediate dose of HDAd-AI (35%, $p < 0.001$, $n=4$). Mice treated with either PBS or the lowest dose of HDAd-AI did not show a significant change in platelet counts (Fig. 3c). Platelet counts returned to pretreatment levels by day 7 in all groups. Thus, the effects of Ad vector treatment on platelets were dose dependent and occurred with both FGAd and HDAd. We detected no significant change in other blood parameters (e.g., WBC, RBC, MCV) among groups (data not shown).

FGAd-AI, not HDAd-AI, induces the appearance of anti-APOA1 antibodies

Newly synthesized APOA1 is a neoantigen and would be predicted to induce an antibody response in APOA1^{-/-} mice. We used immunoblot analysis to analyze for the presence of anti-

APOA1 antibodies in mouse plasma following Ad-AI treatment. Anti-APOA1 antibodies were readily detectable in the plasma of mice treated with FGAd-AI (Fig. 4a, lane 3) but not in that of PBS- or HDAd-AI-treated animals (Fig. 4a, lane 2 and 4). Quantitation of the anti-APOA1 antibody titer by ELISA revealed an absence of anti-APOA1 antibodies in untreated mouse plasma and a marked increase in the anti-APOA1 antibody titer in FGAd-AI-treated mice 14 days after injection, coincident with a rapid decline in plasma APOA1 levels (Fig. 2a and Fig. 4b). The antibody titer reached a maximum of $1:9000 \pm 5300$ dilution at day 42 ($p < 0.05$ vs. pretreatment, $n=5$) and remained markedly elevated ($1:5000 \pm 4900$ dilution, $p < 0.05$ vs. pretreatment) at day 70. In contrast, the plasma anti-APOA1 antibody titer was not significantly changed by HDAd-AI treatment (Fig. 4b).

Co-injection of FGAd suppresses HDAd-mediated APOA1 expression

FGAd vector not only induces T-cell mediated immunity²¹ but also adaptive immunity by its adjuvant effect through induction of cytokine release.^{22,23} In order to test whether FGAd induces a humoral immune response through its adjuvant effect and inhibits HDAd-AI-mediated APOA1 expression, we treated APOA1^{-/-} mice with both HDAd-AI and FGAd vectors and measured the antibody titer. We used human APOE3 gene as an unrelated gene that should not affect the anti-APOA1 antibody titer if the FGAd vector itself has no immunoadjuvant effects; furthermore, APOE3 expression can be differentiated from endogenous mouse APOE by a human specific antibody. The total number of VP injected into mice was adjusted with HDAd-0 (empty vector). The vector structures are summarized in Table 2. Co-injection of 5×10^{11} VP/kg of HDAd-AI and 5×10^{11} VP/kg of HDAd-E3 had no effects on plasma APOA1 levels and cholesterol levels compared with mice treated with HDAd-AI and HDAd-0, while co-injection of FGAd-AI or FGAd-E3 with HDAd-AI markedly attenuated the plasma APOA1 (and cholesterol) response. In mice treated with HDAd-AI and FGAd-E3, plasma APOA1 was undetectable throughout the course of the experiment (Fig. 5a and b). The lack of an APOA1 response in mice treated with either HDAd-AI and FGAd-AI or HDAd-AI and FGAd-E3 was confirmed by immunoblot analysis (Fig. 5c, lane 5 and 8 vs. lane 6) while similar levels of APOA1 were detected in mice treated with HDAd-AI and HDAd-0 or HDAd-AI and HDAd-E3 (Fig. 5c, lane 6 and 7). These data indicate that treatment with FGAd *per se*, regardless of its specific transgene insert or expression, suppresses HDAd-mediated APOA1 expression. However, we detected significant anti-APOA1 antibody titers only in mice treated with HDAd-0 and FGAd-AI or HDAd-AI and FGAd-AI. Interestingly, mice treated with HDAd-AI and FGAd-E3 did not develop anti-APOA1 antibodies (Fig. 5d), an observation that excludes the possibility of an FGAd adjuvant effect *per se* as a cause of inhibition of APOA1 expression.

To obtain a correlation between plasma APOA1 and immunoreactive APOA1 in the liver, we performed APOA1 immunofluorescence in liver sections of mice at day 56. The immunoreactivity was not detected in the liver of mice treated with PBS, HDAd-0 alone, HDAd-AI and FGAd-AI or HDAd-AI and FGAd-E3 (Fig. 6a, b, d and f). In contrast, HDAd-AI and HDAd-E3 treated mice showed a similar level of fluorescence to those treated with HDAd-AI and HDAd-0 (Fig. 6c and e). The significant APOA1 mRNA was not detected in mice co-treated with FGAd vectors by Northern blot analysis (Fig. 6g). To further confirm the presence of APOA1 mRNA in mice treated with FGAd vectors, we performed sensitive RT-PCR. Increasing PCR cycles detected the APOA1 mRNA in the liver of mice treated with HDAd-AI and FGAd vectors but at barely detectable levels compared to those treated with HDAd vectors only (Fig. 6h). The low levels of APOA1 mRNA may be due to low vector copy number. We measured HDAd-AI vector copy number in the liver at day 1 (baseline) and day 56 after treatment by real-time PCR. The copy number fell significantly on day 56 in all groups, but much more so in the FGAd vector co-treated (Fig. 6i, lane 2 and 4) than in HDAd vector co-treated groups (Fig. 6i, lane 1 and 3).

As APOE has been reported to display immunomodulatory properties,^{24,25} we treated mice with a FGAd expressing mouse very-low-density lipoprotein receptor (VLDLR). VLDLR is normally expressed in APOA1^{-/-} mice and its induced overexpression does not induce a humoral immune response.^{10,26} The pattern of plasma cholesterol and APOA1 levels in mice treated with HDAd-AI and FGAd-VLDLR was similar to that in mice treated with HDAd-AI and FGAd-E3. An anti-APOA1 antibody was not detected in mice treated with HDAd-AI and FGAd-VLDLR, and the HDAd-AI vector copy number was 2.8 ± 2.1 copies/diploid genome (n=5) at day 56. Therefore, the suppression of APOA1 expression by FGAd was independent of the transgene expressed.

Long-term phenotypic correction by a single injection of HDAd-AI

As a moderate dose of HDAd-AI produces high plasma APOA1 levels without inducing anti-APOA1 antibodies, we tested the durability of the plasma APOA1 response in APOA1^{-/-} mice. We injected to these mice either PBS or 4.5×10^{12} VP/kg of HDAd-AI and monitored phenotypic correction over a 2 year period. Cholesterol levels in APOA1^{-/-} mice were 10 ± 4 mg/dl (mean \pm SD, n=12) at baseline, compared with 64 ± 12 mg/dl (n= 25) in wild-type C57BL/6 mice. In PBS-injected mice, there was a spontaneous but slow increase in plasma cholesterol level over time to 36 ± 2 mg/dl at the end of two years (day 730), a phenotypic adjustment noted previously.²⁷ In the APOA1^{-/-} mice treated with HDAd-AI, cholesterol levels reached a maximal level of 104 ± 10 mg/dl (n=6) 4 weeks after injection and slowly declined over the next one and a half years to 53 ± 5 mg/dl. At 730 days, plasma cholesterol levels remained higher in all but one HDAd-AI treated mice (58, 49, 27 and 76 mg/dl) than in controls (34 and 37 mg/dl), though the difference was not significant due to the small number of surviving control mice (Fig. 7a). We determined the plasma APOA1 level at day 366 and found it to be undetectable in PBS-treated mice, but 140 ± 55 mg/dl (n=5) in HDAd-AI-treated APOA1^{-/-} mice (normal human APOA1 = 100-150 mg/dl)¹. At 730 days, 3 of the 4 surviving HDAd-AI treated mice had values averaging 61 ± 14 mg/dl. Thus, a moderate dose of HDAd-AI treatment led to high physiological levels of plasma APOA1 that declined to about 50% of the normal level at the end of two years (Fig. 7b). FPLC analysis revealed a prominent HDL cholesterol peak in plasma collected from HDAd-AI-treated mice at 366 and 540 days post-injection. It decreased to about half that of the wild-type mice at 730 days, but was still significantly higher than that in PBS-injected controls (Fig. 7c-e). By immunofluorescence, APOA1 immunoreactivity was detected in 30-40% of the hepatocytes in HDAd-AI-treated mice but was undetectable in PBS-treated controls (Fig. 8d vs. 8c).

Discussion

A variety of problems associated with early generation Ad vectors has made them less than ideal vectors for liver-directed gene therapy. In contrast, HDAds have a significantly better safety profile and duration of transgene expression.^{8,9 10-14} In this study, we compared the acute and chronic toxicities of HDAd and FGAd. Chronic hepatotoxicity caused by leaky Ad viral gene expression manifested by abnormal histopathology occurs with a FGAd, but is eliminated in a HDAd (Fig. 3, Table 1). However, acute toxicity is not significantly different between HDAds and FGAds. For example, dose-related thrombocytopenia occurs with both FGAds and HDAds.^{20,28} The mechanism of Ad-induced thrombocytopenia appears to be multi-faceted and complex. FGAd has been reported to increase platelet clearance.²⁹ Platelets express $\alpha_V\beta_3$ and other integrins that bind to the RGD motif, which is present in the penton base of Ad capsid proteins. However, incubation of platelet-rich human plasma with Ads fails to promote platelet aggregation, and the addition of an Ad vector had no effect on agonist-induced aggregation *in vitro*.³⁰ Finally, intravenous injection of lethal doses of FGAd in nonhuman primates causes diffuse endothelial damage that may lead to platelet activation, aggregation and depletion.^{19,31}

There is a nonlinear dose response to Ad vector transgene expression.³²⁻³⁵ Sequestration of an Ad vector by Kupffer cells may underlie this threshold effect.³⁵ Following systemic administration, Ads are taken up by macrophages, Kupffer cells, before they are taken up by hepatocytes.^{33,35} An acute cytokine response to systemic Ad vector administration in mice has been reported to be mediated by dendritic cells (DCs) and macrophages.³⁶ Thus, depletion of DCs or macrophages before therapeutic Ad administration is one strategy to reduce vector-associated acute toxicity as well as to increase hepatic transduction efficiency.³⁷ The enhancement of hepatocyte transduction has also been reported after pre-administration of an unrelated Ad presumably to saturate the non-hepatic Ad binding sites.³⁵

A previous study using an HDAd containing an APOE gene demonstrated a lifetime phenotypic correction of a genetic APOE deficiency in mice.¹¹ The current study aims to correct a heritable APOA1 deficiency, a much more common disorder, by APOA1 gene transfer. In these two apolipoprotein deficiency models, the newly synthesized transgene products are neoantigens. It is unclear how treated mice exhibit immuno-tolerance towards neoantigens, permitting unattenuated long-term transgene expression after HDAd-AI delivery. C57BL/6 mice have been reported to be more immuno-tolerant than other strains.^{38,39} However, FGAd-AI-treated C57BL/6 mice develop anti-APOA1 antibodies, indicating that they can mount a humoral immune response. One potential explanation for the transient nature of transgene expression of FGAd-AI and the FGAd-AI-mediated suppression of HDAd-AI vector-mediated APOA1 expression is an FGAd-mediated adjuvant effect via cytokine release.²² Our experiment co-injecting HDAd-AI and FGAd-E3 rules out an adjuvant effect of FGAd *per se* as the explanation. Also refuting the possibility of an adjuvant effect by FGAds is the good level of APOE3 expression 56 days after FGAd-E3 treatment (Fig. 5c).

HDAds have been shown to have an attenuated adaptive immune response compared with FGAds.⁴⁰ De Geest et al have reported the strict dependence of mouse humoral anti-APOA1 immune response on APOA1 expression in antigen-presenting cells.⁴¹ Although the experimental design of the current study differs from those of previous reports using wild-type C57/BL6 mice in which APOA1 is not a neoantigen,⁴¹⁻⁴³ our data support the notion that antigen presentation in APCs is required to induce a humoral response against APOA1. Our study also corroborates reports indicating that the use of a liver-specific promoter that avoids expression in antigen presenting cells reduces the immune response towards transgene products.^{42,44}

Although co-injection of FGAd-E3 or FGAd-VLDLR with HDAd-AI failed to induce an anti-APOA1 antibody in APOA1^{-/-} mice, these FGAds decreased the HDAd vector copy number. 11-15 % of vector DNA were present in these mice compared to control mice (Figure 6i). Substantial transgene expression, despite accelerated loss of vector DNA, has been reported in HDAd-mediated dystrophin expression in *mdx* mice.⁴⁵ Therefore, undetectable APOA1 expression in liver and in plasma of mice treated with both HDAd-AI and a FGAd vector was unexpected in the absence of APOA1 neutralizing antibodies (Fig 6g). In addition to reduced vector copy number, FGAd genome or CMV promoter used in these vectors may have further inhibited transcription of the human APOA1 gene. Bacterial DNA sequences have been suggested to play a role in episomal transgene silencing in a nonviral vector which is mediated by a covalent linkage of the expression cassette and the bacterial DNA elements.^{46,47} Although promoter silencing of nonviral DNA was promoter/enhancer independent, we found that it was promoter-dependent in the current study. Substantial APOE3 expression driven by CMV promoter was evident in mice treated with HDAd-AI and FGAd-E3 56 days after treatment, while APOA1 expression was undetectable (Fig. 5c, lane 8). DNA of a FGAd vector may function as an insulator or a low-level leaky expression of FGAd gene may interfere with the transcription of episomal transgene expression driven by a mammalian promoter. Alternatively, competition of a viral promoter with APOA1 promoter is in play.⁴⁸ Data

supporting this notion has been reported by Wen et al. who found enhanced but not suppressed HDAd vector-mediated urokinase plasminogen activator expression following FGAd co-administration in which the transgene delivered by HDAd vector was driven by CMV promoter.⁴⁹

Due to the adverse events of integrating viral vectors, non-integrating viral vectors such as Ad vector have emerged as a preferred vector for some gene therapy applications. Although the frequency of chromosomal integration of an HDAd vector has been reported to be slightly higher than that of a FGAd,^{50,51} HDAds are essentially non-integrating vectors, and transgene expression is eventually eliminated with repeated cell divisions. Despite long-term phenotypic correction, the plasma APOA1 level declined from supraphysiological level at 4 weeks to 50% of normal level over 2 years. We previously showed that the same HDAd produced with helper viruses of different serotypes can re-stimulate transgene expression. By alternating serotypes, a therapeutic level of transgene expression can be maintained for an extended time period.¹¹

In summary, we have demonstrated that a single injection of a modest dose of HDAd expressing human APOA1 gene corrects the phenotype almost for a lifetime in a mouse model of hypoalphalipoproteinemia with an improved safety profile. Further studies examining the safety and efficacy of HDAd-mediated APOA1 gene therapy in large animal models are warranted.

Materials and methods

Recombinant adenoviral vectors

The HDAd-AI contains the 11-kb EcoRI fragment of the human APOA1 gene, including the 5.5 kb of 5' and 3.5 kb of 3' flanking DNA on a p Δ 21 backbone.¹¹ Rescue and amplification of the HDAd-AI were performed by the method of Parks et al.⁵² The absence of DNA rearrangement and helper virus contamination were analyzed by Southern blot. Human APOA1 cDNA was cloned into a KS vector by reverse transcription-PCR using total cellular RNA prepared from HepG2 cells. The following primers were used: 5'-GAA GGA TCC ACC ATG AAA GCT GCG GTG CTG AC-3' and 5'-AAG GAA TTC ACT GGG TGT TGA GCT TCT-3'. They contained artificial cloning sites (underlined) and the Kozak sequence (bold faced) at the translation initiation codon. The nucleotide sequence was verified by DNA sequence analysis, and the APOA1 cDNA was subcloned into the pAvCvSv shuttle vector.⁵³ FGAd-AI was produced by standard techniques. Both vectors were produced on serotype 5. Human apoE3 expressing Ad vectors were produced using human APOE3 cDNA or an 11-kb Hind III fragment containing APOE3 gene and the liver enhancer element.¹¹ A FGAd expressing mouse very low density lipoprotein receptor (VLDLR) has been described.¹⁰ HDAd-0 (empty vector) was made on pC4HSU backbone.⁵⁴ The infectious titer of FGAd-AI was determined by a standard plaque assay, and that of HDAd-AI was determined by a DNA-based method described by Kreppel et al.⁵⁵ The infectious unit/vector particle ratios of FGAd-AI and HDAd-AI were 1:20 and 1: 17, respectively.

Animal studies

Female APOA1^{-/-} mice on a C57BL/6 background were purchased from Jackson Laboratories and were kept on a regular chow diet. Experiments were performed at 9-13 weeks of age with an average weight of 20 grams. To conduct the dose-response study, mice (4-5 per group) were injected via tail vein with PBS; HDAd-AI at escalating doses: 5×10^{11} vector particles (VP)/kg, 1.5×10^{12} VP/kg and 4.5×10^{12} VP/kg; or FGAd-AI at a dose of 4.5×10^{12} VP/kg. For liver pathology, mice were treated with PBS alone or with 4.5×10^{12} VP/kg of HDAd-AI or FGAd-AI, and two mice per group were sacrificed at various times. For co-injection, 5×10^{12} VP/kg of HDAd and FGAd vectors were injected. The total number of Ad vectors injected

(1×10^{13} VP/kg) was adjusted with HDAd-0 (empty vector). Long-term transgene expression was evaluated for up to 2 years after the virus treatment at the dose of 4.5×10^{12} VP/kg. A control group received PBS. For plasma determinations, mice were fasted for 5 hours, anesthetized with methoxyfluorane or isofluorane, and blood was collected in EDTA by puncturing the saphenous vein or the retro-orbital plexus.^{10,11}

Phenotype analysis

Cholesterol and FPLC analyses were performed as previously described.¹⁰ Plasma human APOA1 levels were quantified by an immunoturbidometric assay adapted for a 96-well plate format (Diasorin). HDL cholesterol was determined by FPLC. Two or three sets of pooled plasma (200 μ l) from control and HDAd-AI-treated mice were used for these determinations. For human APOA1 immunoblot analysis, plasma was diluted 1:32, electrophoresed on a 12% SDS-polyacrylamide gel, and transferred to a nitrocellulose membrane. The membrane was then incubated with a goat anti-human APOA1 antibody (1:2000 dilution, Chemicon) with detection using ECL (Amersham Pharmacia Biotech). For APOE3 immunoblot, goat anti-APOE antibody (1:4000, Calbiochem) or mouse monoclonal anti-human APOE3 (1:1000, SIGNET Lab) were used.

Immunohistochemistry

Approximately 3 mm thick sections of the left-lateral lobe of the liver were embedded in O.C.T. and stored at -80°C . Cryosections (5 μm -thick) were fixed in cold acetone at -20°C for 5 min, blocked with 1% BSA for 1h, and used for immunofluorescence staining. The sections were incubated with a goat anti-human APOA1 antibody (1:100) in 1% BSA for 30 min at 37°C , washed with PBS (pH 7.2), and incubated with rabbit anti-goat antibody conjugated to Alexa Fluor 488 (1:200, Molecular Probes). The slides were mounted with Vectashield[®] Mounting Medium with DAPI (Vector Laboratories), and the images were captured with the Axioplan 2 microscope and Axiovision 4.1 software (Carl Zeiss).

Toxicity studies

Histological analyses were performed on formalin-fixed, paraffin-embedded tissues as previously described¹⁸. ALT activity and whole blood counts were determined on fresh samples by the Clinical Pathology Laboratory in the Center for Comparative Medicine at Baylor College of Medicine (Houston, TX).

Detection of anti-human APOA1 antibodies

For detection of an anti-APO1 antibody by immunoblot assay, 1.4 μg of purified human HDL were separated on a 4-20% SDS-PAGE, transferred to a nitrocellulose membrane, and incubated with plasma collected from mice treated with Ad vectors as a primary antibody (1:1000). The anti-human APOA1 antibody titer was also determined by direct ELISA. A flat bottom 96-well EIA/RIA medium binding plate (Costar) was coated with 50 μl of purified human HDL (Calbiochem, 200 ng/well) at 4°C overnight. After washing the plate with 20 mM Tris buffered saline pH7.5 (TBS) containing 0.05% Tween 20 (TBS-T), the plate was blocked with TBS-T containing 4% skim milk, and incubated with plasma diluted with TBS-T. After washing, the plate was incubated with 50 μl of peroxidase conjugated goat anti-mouse IgG (Pierce, 1:1000 dilution with 0.1x blocking solution). The plate was washed and incubated with 100 μl of substrate (Pierce 1-Step Turbo TMB-ELISA) for 30 min at room temperature while being protected from light. The reaction was terminated by an addition of 100 μl of 1M H_2SO_4 solution, and the plate was read at 450 nm. The titer of antibodies was defined as the reciprocal of the highest dilution giving an optical density of 0.1 at 450 nm.

Northern blot and RT-PCR analyses

Total cellular RNA was prepared using TRIzol reagent (Invitrogen). Twenty μ g of RNA was electrophoresed on a 1.2% formaldehyde/agarose gel, transferred to a nylon membrane, and hybridized to a 32 P labeled-0.8 kb human APOA1 cDNA probe. For RT-PCR, the following primers were used: 5'- ATT GTT GCC ATC AAC GAC CC - 3' and 5' -CCA CGA CAT ACT CAG CAC C - 3' for mouse GAPDH mRNA; 5' - ACGTGGATGTGCTCAAAGACAG - 3' and 5' - ATCCTTGCTCATCTCTTGCCCTC - 3' for human APOA1 mRNA.

Detection of adenoviral vector genomes in tissue samples

Ad vector DNA was obtained from the liver using DNA kit (Qiagen) and the vector copy number was determined by quantitative real-time PCR of the vector backbones using SYBR Green QPCR master mix (Bio-Rad). The PCR primers for p Δ 21 based HDAd vectors were: 5' - TTGGGCGTAACCGAGTAAG - 3' and 5' -ACTTCCTACCCATAAGCTCC - 3'.

Statistics

Statistical analyses on lipid data were performed by two-way analysis of variance (ANOVA) with factors time and treatment group (HDAd-AI vs. control) or by one-way ANOVA using SigmaStat (SYSTAT Software Co.). Statistical significance was assigned at $p < 0.05$.

Acknowledgements

This work was supported by HL59314 and HL73144. A. Paul was supported by the grant from American Heart Association (0535118N). We thank A. Beudet for valuable discussion; S. Kochanek and G. Shiedner for providing 293Cre66 cells; J. Smith for APOE gene; F. Graham for providing helper virus; Merck & Co. for providing reagents developed by F. Graham.

References

- Schaefer EJ, Lamon-Fava S, Ordovas JM, Cohn SD, Schaefer MM, Castelli WP, et al. Factors associated with low and elevated plasma high density lipoprotein cholesterol and apolipoprotein A-I levels in the Framingham Offspring Study. *J Lipid Res* 1994;35:871–882. [PubMed: 8071609]
- Kannel WB. Range of serum cholesterol values in the population developing coronary artery disease. *Am J Cardiol* 1995;76:69C–77C.
- Gordon DJ, Rifkind BM. High-density lipoprotein--the clinical implications of recent studies. *N Engl J Med* 1989;321:1311–1316. [PubMed: 2677733]
- Maciejko JJ, Holmes DR, Kottke BA, Zinsmeister AR, Dinh DM, Mao SJ. Apolipoprotein A-I as a marker of angiographically assessed coronary-artery disease. *N Engl J Med* 1983;309:385–389. [PubMed: 6410239]
- Schaefer EJ, Heaton WH, Wetzel MG, Brewer HB Jr. Plasma apolipoprotein A-1 absence associated with a marked reduction of high density lipoproteins and premature coronary artery disease. *Arteriosclerosis* 1982;2:16–26. [PubMed: 6800349]
- Forte TM, Nichols AV, Krauss RM, Norum RA. Familial apolipoprotein AI and apolipoprotein CIII deficiency. Subclass distribution, composition, and morphology of lipoproteins in a disorder associated with premature atherosclerosis. *J Clin Invest* 1984;74:1601–1613. [PubMed: 6501564]
- Yamakawa-Kobayashi K, Yanagi H, Fukayama H, Hirano C, Shimakura Y, Yamamoto N, et al. Frequent occurrence of hypoalphalipoproteinemia due to mutant apolipoprotein A-I gene in the population: a population-based survey. *Hum Mol Genet* 1999;8:331–336. [PubMed: 9931341]
- Schiedner G, Morral N, Parks RJ, Wu Y, Koopmans SC, Langston C, et al. Genomic DNA transfer with a high-capacity adenovirus vector results in improved in vivo gene expression and decreased toxicity. *Nat Genet* 1998;18:180–183. [PubMed: 9462752]
- Morral N, O'Neal W, Rice K, Leland M, Kaplan J, Piedra PA, et al. Administration of helper-dependent adenoviral vectors and sequential delivery of different vector serotype for long-term liver-directed gene transfer in baboons. *Proc Natl Acad Sci U S A* 1999;96:12816–12821. [PubMed: 10536005]

10. Oka K, Pastore L, Kim IH, Merched A, Nomura S, Lee HJ, et al. Long-term stable correction of low-density lipoprotein receptor-deficient mice with a helper-dependent adenoviral vector expressing the very low-density lipoprotein receptor. *Circulation* 2001;103:1274–1281. [PubMed: 11238273]
11. Kim IH, Jozkowicz A, Piedra PA, Oka K, Chan L. Lifetime correction of genetic deficiency in mice with a single injection of helper-dependent adenoviral vector. *Proc Natl Acad Sci U S A* 2001;98:13282–13287. [PubMed: 11687662]
12. Belalcazar LM, Merched A, Carr B, Oka K, Chen KH, Pastore L, et al. Long-term stable expression of human apolipoprotein A-I mediated by helper-dependent adenovirus gene transfer inhibits atherosclerosis progression and remodels atherosclerotic plaques in a mouse model of familial hypercholesterolemia. *Circulation* 2003;107:2726–2732. [PubMed: 12742997]
13. Brunetti-Pierri N, Nichols TC, McCorquodale S, Merricks E, Palmer DJ, Beaudet AL, et al. Sustained phenotypic correction of canine hemophilia B after systemic administration of helper-dependent adenoviral vector. *Hum Gene Ther* 2005;16:811–820. [PubMed: 16000063]
14. Toietta G, Mane VP, Norona WS, Finegold MJ, Ng P, McDonagh AF, et al. Lifelong elimination of hyperbilirubinemia in the Gunn rat with a single injection of helper-dependent adenoviral vector. *Proc Natl Acad Sci U S A* 2005;102:3930–3935. [PubMed: 15753292]
15. Nomura S, Merched A, Nour E, Dieker C, Oka K, Chan L. Low-density lipoprotein receptor gene therapy using helper-dependent adenovirus produces long-term protection against atherosclerosis in a mouse model of familial hypercholesterolemia. *Gene Ther* 2004;11:1540–1548. [PubMed: 15269711]
16. De Geest B, Zhao Z, Collen D, Holvoet P. Effects of adenovirus-mediated human apo A-I gene transfer on neointima formation after endothelial denudation in apo E-deficient mice. *Circulation* 1997;96:4349–4356. [PubMed: 9416903]
17. Raper SE, Yudkoff M, Chirmule N, Gao GP, Nunes F, Haskal ZJ, et al. A pilot study of in vivo liver-directed gene transfer with an adenoviral vector in partial ornithine transcarbamylase deficiency. *Hum Gene Ther* 2002;13:163–175. [PubMed: 11779420]
18. O'Neal WK, Zhou H, Morral N, Aguilar-Cordova E, Pestaner J, Langston C, et al. Toxicological comparison of E2a-deleted and first-generation adenoviral vectors expressing alpha1-antitrypsin after systemic delivery. *Hum Gene Ther* 1998;9:1587–1598. [PubMed: 9694157]
19. Morral N, O'Neal WK, Rice K, Leland MM, Piedra PA, Aguilar-Cordova E, et al. Lethal toxicity, severe endothelial injury, and a threshold effect with high doses of an adenoviral vector in baboons. *Hum Gene Ther* 2002;13:143–154. [PubMed: 11779418]
20. Brunetti-Pierri N, Palmer DJ, Beaudet AL, Carey KD, Finegold M, Ng P. Acute toxicity after high-dose systemic injection of helper-dependent adenoviral vectors into nonhuman primates. *Hum Gene Ther* 2004;15:35–46. [PubMed: 14965376]
21. Yang Y, Nunes FA, Berencsi K, Furth EE, Gonczol E, Wilson JM. Cellular immunity to viral antigens limits E1-deleted adenoviruses for gene therapy. *Proc Natl Acad Sci U S A* 1994;91:4407–4411. [PubMed: 8183921]
22. Higginbotham JN, Seth P, Blaese RM, Ramsey WJ. The release of inflammatory cytokines from human peripheral blood mononuclear cells in vitro following exposure to adenovirus variants and capsid. *Hum Gene Ther* 2002;13:129–141. [PubMed: 11779417]
23. Tatsis N, Ertl HC. Adenoviruses as vaccine vectors. *Mol Ther* 2004;10:616–629. [PubMed: 15451446]
24. Kelly ME, Clay MA, Mistry MJ, Hsieh-Li HM, Harmony JA. Apolipoprotein E inhibition of proliferation of mitogen-activated T lymphocytes: production of interleukin 2 with reduced biological activity. *Cell Immunol* 1994;159:124–139. [PubMed: 7994749]
25. van den Elzen P, Garg S, Leon L, Brigl M, Leadbetter EA, Gumperz JE, et al. Apolipoprotein-mediated pathways of lipid antigen presentation. *Nature* 2005;437:906–910. [PubMed: 16208376]
26. Kozarsky KF, Jooss K, Donahee M, Strauss JF 3rd, Wilson JM. Effective treatment of familial hypercholesterolaemia in the mouse model using adenovirus-mediated transfer of the VLDL receptor gene. *Nat Genet* 1996;13:54–62. [PubMed: 8673104]
27. Plump AS, Azrolan N, Odaka H, Wu L, Jiang X, Tall A, et al. ApoA-I knockout mice: characterization of HDL metabolism in homozygotes and identification of a post-RNA mechanism of apoA-I up-regulation in heterozygotes. *J Lipid Res* 1997;38:1033–1047. [PubMed: 9186920]

28. Toietta G, Pastore L, Cerullo V, Finegold M, Beaudet AL, Lee B. Generation of helper-dependent adenoviral vectors by homologous recombination. *Mol Ther* 2002;5:204–210. [PubMed: 11829528]
29. Wolins N, Lozier J, Eggerman TL, Jones E, Aguilar-Cordova E, Vostal JG. Intravenous administration of replication-incompetent adenovirus to rhesus monkeys induces thrombocytopenia by increasing in vivo platelet clearance. *Br J Haematol* 2003;123:903–905. [PubMed: 14632782]
30. Eggerman TL, Mondoro TH, Lozier JN, Vostal JG. Adenoviral vectors do not induce, inhibit, or potentiate human platelet aggregation. *Hum Gene Ther* 2002;13:125–128. [PubMed: 11779416]
31. Lozier JN, Csako G, Mondoro TH, Krizek DM, Metzger ME, Costello R, et al. Toxicity of a first-generation adenoviral vector in rhesus macaques. *Hum Gene Ther* 2002;13:113–124. [PubMed: 11779415]
32. Morral N, Parks RJ, Zhou H, Langston C, Schiedner G, Quinones J, et al. High doses of a helper-dependent adenoviral vector yield supraphysiological levels of alpha1-antitrypsin with negligible toxicity. *Hum Gene Ther* 1998;9:2709–2716. [PubMed: 9874269]
33. Bristol JA, Shirley P, Idamakanti N, Kaleko M, Connelly S. In vivo dose threshold effect of adenovirus-mediated factor VIII gene therapy in hemophilic mice. *Mol Ther* 2000;2:223–232. [PubMed: 10985953]
34. Ziegler RJ, Li C, Cherry M, Zhu Y, Hempel D, van Rooijen N, et al. Correction of the nonlinear dose response improves the viability of adenoviral vectors for gene therapy of Fabry disease. *Hum Gene Ther* 2002;13:935–945. [PubMed: 12031126]
35. Tao N, Gao GP, Parr M, Johnston J, Baradet T, Wilson JM, et al. Sequestration of adenoviral vector by Kupffer cells leads to a nonlinear dose response of transduction in liver. *Mol Ther* 2001;3:28–35. [PubMed: 11162308]
36. Zhang Y, Chirmule N, Gao GP, Qian R, Croyle M, Joshi B, et al. Acute cytokine response to systemic adenoviral vectors in mice is mediated by dendritic cells and macrophages. *Mol Ther* 2001;3:697–707. [PubMed: 11356075]
37. Schiedner G, Hertel S, Johnston M, Dries V, van Rooijen N, Kochanek S. Selective depletion or blockade of Kupffer cells leads to enhanced and prolonged hepatic transgene expression using high-capacity adenoviral vectors. *Mol Ther* 2003;7:35–43. [PubMed: 12573616]
38. Fields PA, Armstrong E, Hagstrom JN, Arruda VR, Murphy ML, Farrell JP, et al. Intravenous administration of an E1/E3-deleted adenoviral vector induces tolerance to factor IX in C57BL/6 mice. *Gene Ther* 8:354–361. [PubMed: 11313811]
39. Kung SH, Hagstrom JN, Cass D, Tai SJ, Lin HF, Stafford DW, et al. Human factor IX corrects the bleeding diathesis of mice with hemophilia B. *Blood* 1998;91:784–790. [PubMed: 9446637]
40. Muruve DA, Cotter MJ, Zaiss AK, White LR, Liu Q, Chan T, et al. Helper-dependent adenovirus vectors elicit intact innate but attenuated adaptive host immune responses in vivo. *J Virol* 2004;78:5966–5972. [PubMed: 15140994]
41. De Geest BR, Van Linthout SA, Collen D. Humoral immune response in mice against a circulating antigen induced by adenoviral transfer is strictly dependent on expression in antigen-presenting cells. *Blood* 2003;101:2551–2556. [PubMed: 12446451]
42. De Geest B, Van Linthout S, Lox M, Collen D, Holvoet P. Sustained expression of human apolipoprotein A-I after adenoviral gene transfer in C57BL/6 mice: role of apolipoprotein A-I promoter, apolipoprotein A-I introns, and human apolipoprotein E enhancer. *Hum Gene Ther* 2000;11:101–112. [PubMed: 10646643]
43. De Geest B, Van Linthout S, Collen D. Sustained expression of human apo A-I following adenoviral gene transfer in mice. *Gene Ther* 2001;8:121–127. [PubMed: 11313781]
44. Pastore L, Morral N, Zhou H, Garcia R, Parks RJ, Kochanek S, et al. Use of a liver-specific promoter reduces immune response to the transgene in adenoviral vectors. *Hum Gene Ther* 1999;10:1773–1781. [PubMed: 10446917]
45. Dudley RW, Lu Y, Gilbert R, Matecki S, Nalbantoglu J, Petrof BJ, et al. Sustained improvement of muscle function one year after full-length dystrophin gene transfer into mdx mice by a gutted helper-dependent adenoviral vector. *Hum Gene Ther* 2004;15:145–156. [PubMed: 14975187]
46. Chen ZY, He CY, Meuse L, Kay MA. Silencing of episomal transgene expression by plasmid bacterial DNA elements in vivo. *Gene Ther* 2004;11:856–864. [PubMed: 15029228]

47. Ehrhardt A, Xu H, Huang Z, Engler JA, Kay MA. A direct comparison of two nonviral gene therapy vectors for somatic integration: in vivo evaluation of the bacteriophage integrase phiC31 and the Sleeping Beauty transposase. *Mol Ther* 2005;11:695–706. [PubMed: 15851008]
48. Polansky, H. Microcompetition with foreign DNA and the origin of chronic disease. The Center for the Biology and Chronic Disease; Rochester: 2003.
49. Wen S, Graf S, Massey PG, Dichek DA. Improved vascular gene transfer with a helper-dependent adenoviral vector. *Circulation* 2004;110:1484–1491. [PubMed: 15326058]
50. Harui A, Suzuki S, Kochanek S, Mitani K. Frequency and stability of chromosomal integration of adenovirus vectors. *J Virol* 1999;73:6141–6146. [PubMed: 10364373]
51. Hillgenberg M, Tonnies H, Strauss M. Chromosomal integration pattern of a helper-dependent minimal adenovirus vector with a selectable marker inserted into a 27.4-kilobase genomic stuffer. *J Virol* 2001;75:9896–9908. [PubMed: 11559822]
52. Parks RJ, Chen L, Anton M, Sankar U, Rudnicki MA, Graham FL. A helper-dependent adenovirus vector system: removal of helper virus by Cre-mediated excision of the viral packaging signal. *Proc Natl Acad Sci U S A* 1996;93:13565–13570. [PubMed: 8942974]
53. Kobayashi K, Oka K, Forte T, Ishida B, Teng B, Ishimura-Oka K, et al. Reversal of hypercholesterolemia in low density lipoprotein receptor knockout mice by adenovirus-mediated gene transfer of the very low density lipoprotein receptor. *J Biol Chem* 1996;271:6852–6860. [PubMed: 8636110]
54. Sandig V, Youil R, Bett AJ, Franlin LL, Oshima M, Maione D, et al. Optimization of the helper-dependent adenovirus system for production and potency in vivo. *Proc Natl Acad Sci U S A* 2000;97:1002–1007. [PubMed: 10655474]
55. Kreppel F, Biermann V, Kochanek S, Schiedner G. A DNA-based method to assay total and infectious particle contents and helper virus contamination in high-capacity adenoviral vector preparations. *Hum Gene Ther* 2002;13:1151–1156. [PubMed: 12133268]

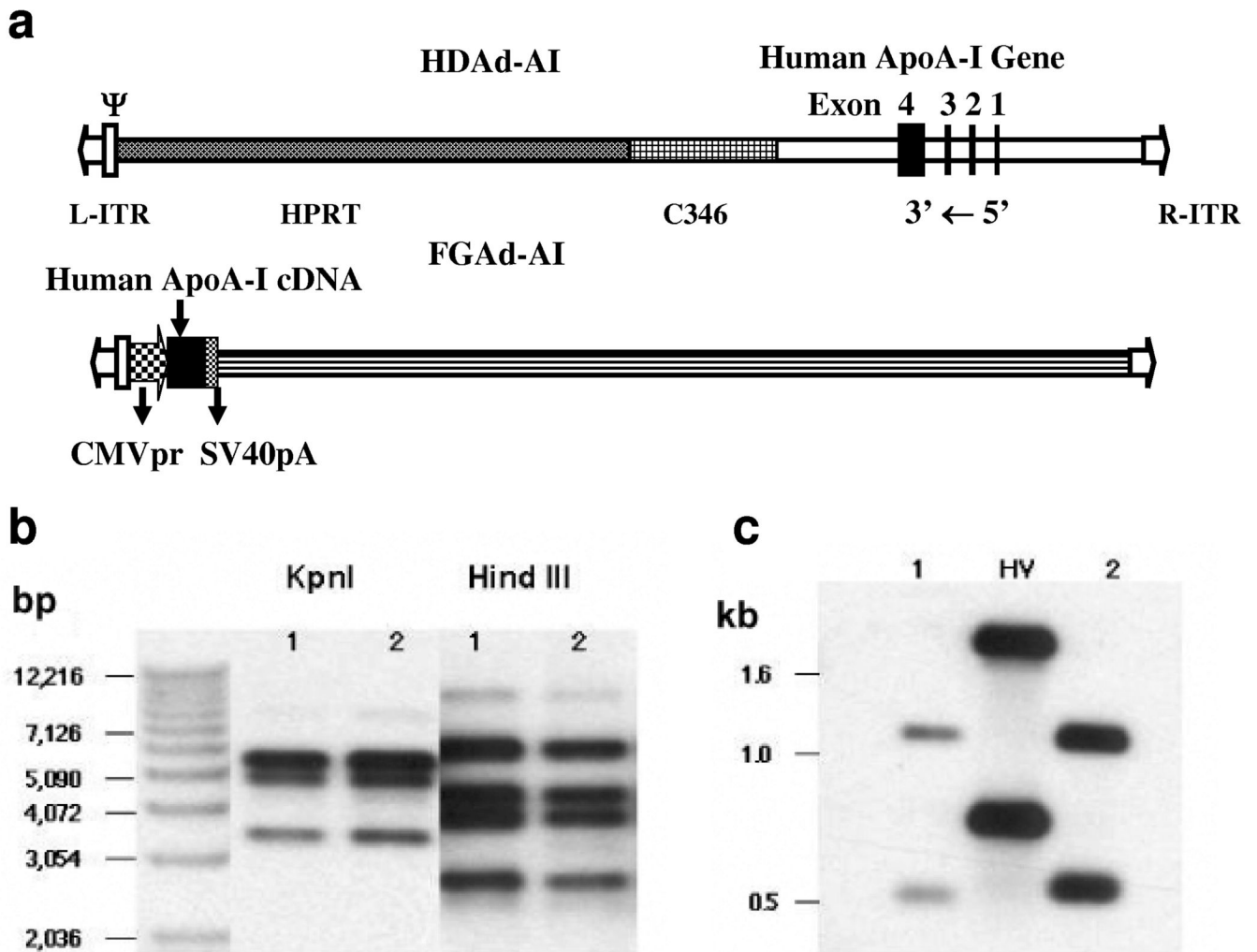


Figure 1.

Structures and characterization of Ad vectors. (a) Structure of HDAd-AI and FGAd-AI. L-ITR and R-ITR: left and right Ad inverted terminal repeat; ψ : Ad packaging signal; HPRT: intron region of human hypoxanthine phosphoribosyltransferase gene; C346: cosmid C346 human genomic stuffer sequence; CMVpr: CMV promoter; SV40pA; SV40 polyadenylation signal. (b) Restriction enzyme mapping of shuttle and HDAd-AI vector. The probe was p Δ 21-APOA1 without the plasmid backbone. (c) Analysis of helper virus contamination. The DNAs were digested with Pst I and hybridized to the L-ITR plus the packaging signal sequence. Lane 1: Pme I digested p Δ 21-APOAI plasmid; Lane 2: HDAd-AI; HV: helper virus.

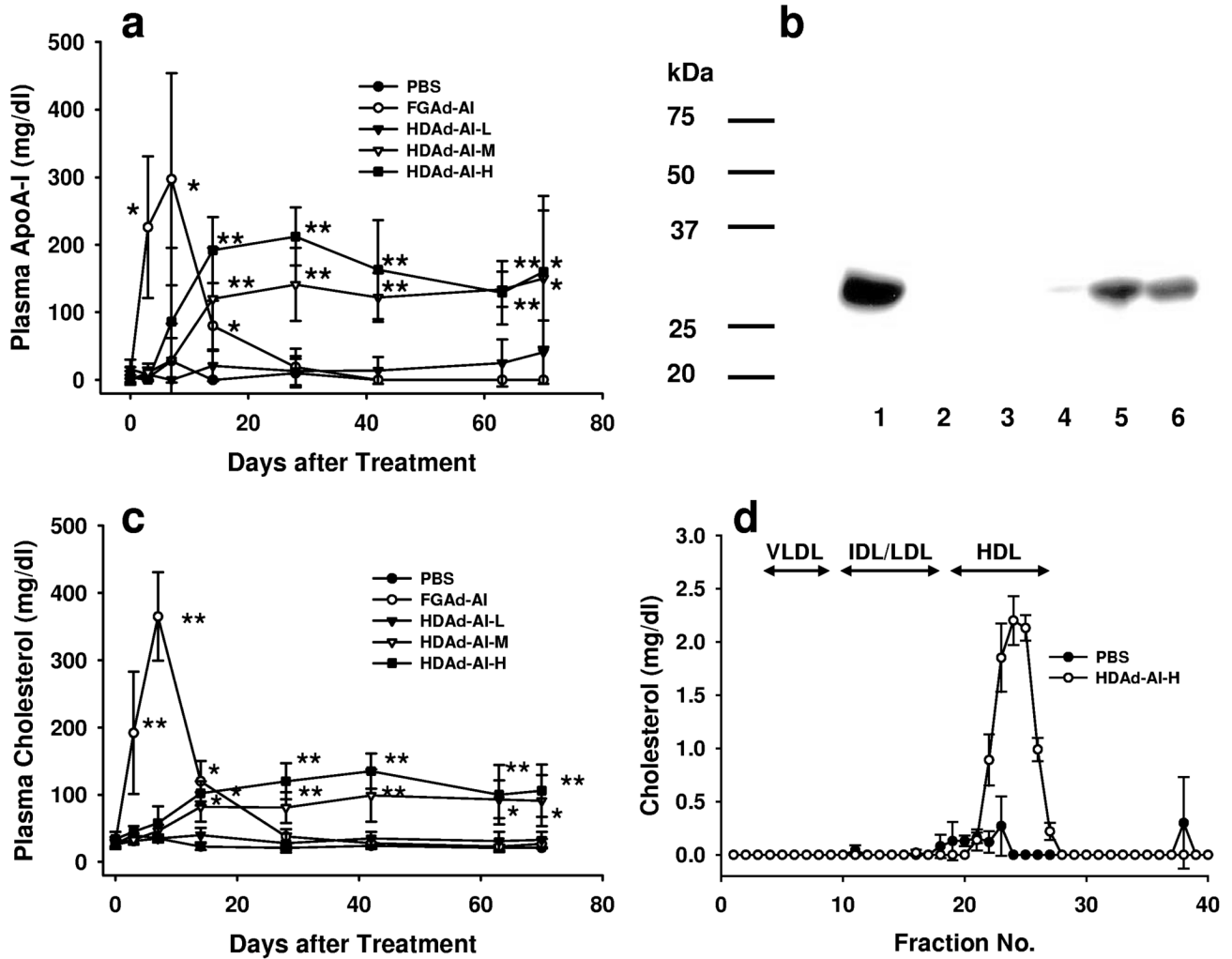


Figure 2.

Comparison of FGAd and HDAd vectors. (a) Plasma human APOA1 levels in APOA1^{-/-} mice following intravenous administration of Ad vectors. HDAd-AI-L: 5×10^{11} VP/kg; HDAd-AI-M: 1.5×10^{12} VP/kg and HDAd-AI-H: 4.5×10^{12} VP/kg; FGAd-AI: 4.5×10^{12} VP/kg. * $p < 0.05$, ** $p < 0.01$. (b) Immunoblots of hAPOA1 in plasma of APOA1^{-/-} mice 84 days after Ad vector treatment. Goat anti-human APOA1 antibody was used (1:2000). Lane 1: human plasma; lane 2: PBS; lane 3: FGAd-AI; lane 4: HDAd-AI-L; lane 5: HDAd-AI-M; lane 6: HDAd-AI-H. (c) Plasma cholesterol levels. * $p < 0.05$, ** $p < 0.01$. (d) Plasma lipoprotein profile. Plasma was collected from the mice 84 days after a single injection of 4.5×10^{12} VP/kg of HDAd-AI or PBS and the lipoproteins were separated on FPLC. Values are mean \pm SD (n=3 per group).

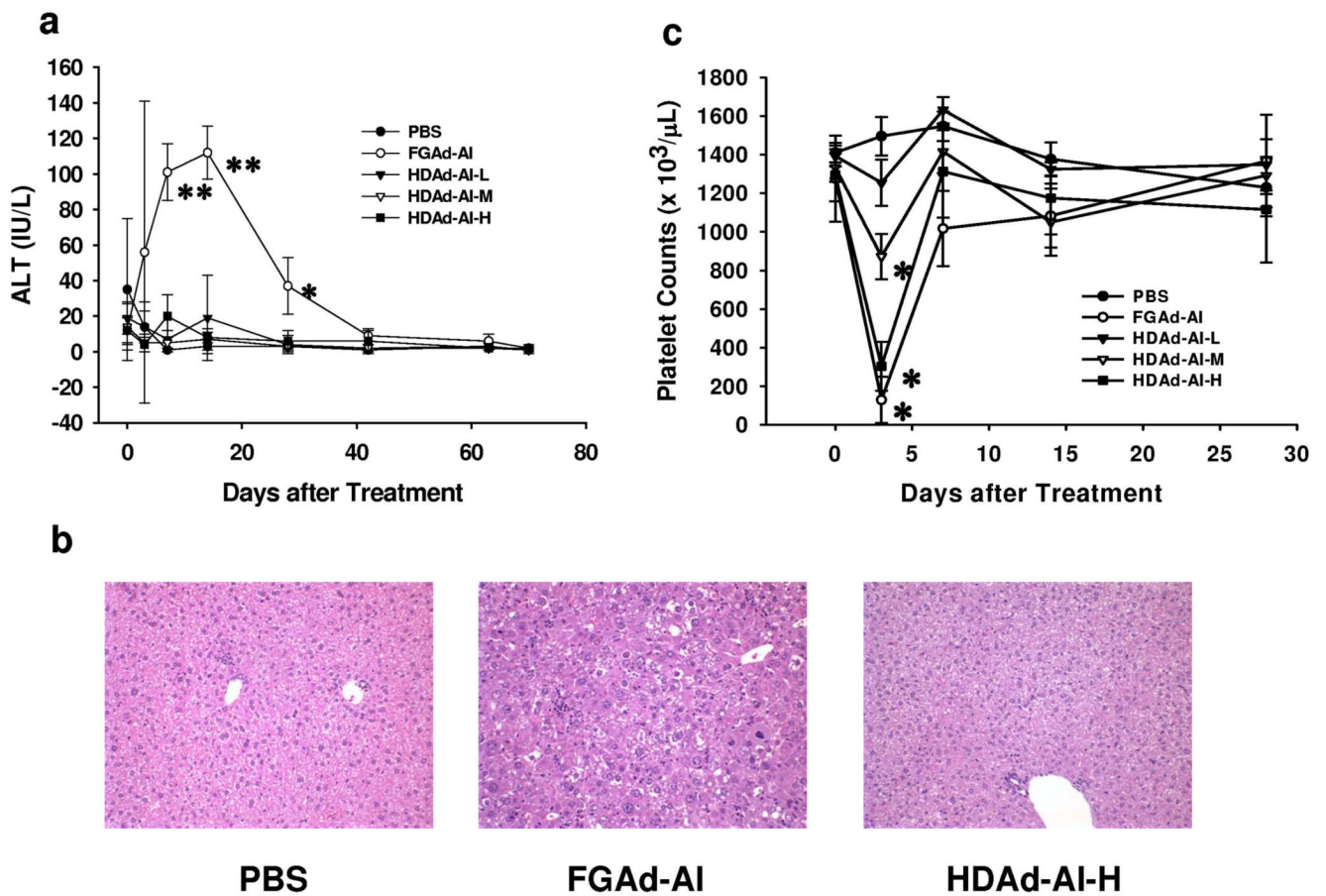


Figure 3. Toxicity associated with intravenous injection of Ad vectors. (a) Plasma ALT activities after Ad vector treatment. HDAd-AI-L: 5×10^{11} VP/kg; HDAd-AI-M: 1.5×10^{12} VP/kg and HDAd-AI-H: 4.5×10^{12} VP/kg; FGAd-AI: 4.5×10^{12} VP/kg. ** $p < 0.001$, * $p < 0.05$ (vs. before treatment) (b) Liver histology. Histopathological analysis was determined by hematoxylin and eosin staining of paraffin embedded liver sections collected 8 days after treatment. See Table 1 for details. (c) Platelet counts. * $p < 0.001$ (vs. pretreatment).

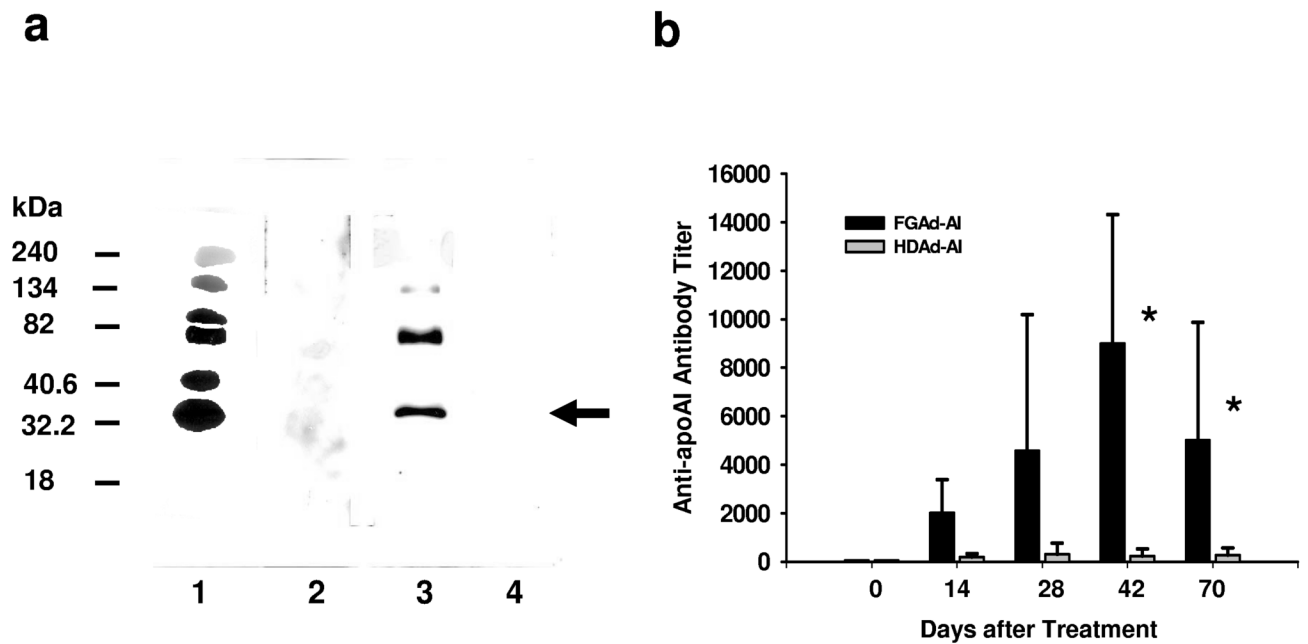


Figure 4.

APOA1 gene therapy for genetic deficiency of APOA1 mediated by FGAd but not HDAd vector produced anti-APOA1 antibodies. (a) Immunoblot analysis. The purified human HDL (1 μ g) was blotted on the membrane and incubated with plasma (1:1000) collected from APOA1^{-/-} mice 6 weeks after treatment with 4.5×10^{12} VP/kg of Ad vectors. The presence of anti-hAPOA1 was detected by ECL. Lane 1: goat anti-hAPOA1 (positive control); lane 2: PBS; lane 3: FGAd-AI; lane 4: HDAd-AI-H. Arrow indicates human APOA1. (b) Anti-hAPOA1 antibody titer in mouse plasma after treatment with Ad vectors. APOA1^{-/-} mice were treated with either FGAd-AI or HDAd-AI at the dose of 4.5×10^{12} VP/kg. Antibody titer is expressed as reciprocal dilutions for which OD_{450 nm} is 0.1 in the assay. *p<0.05 (vs. pretreatment).

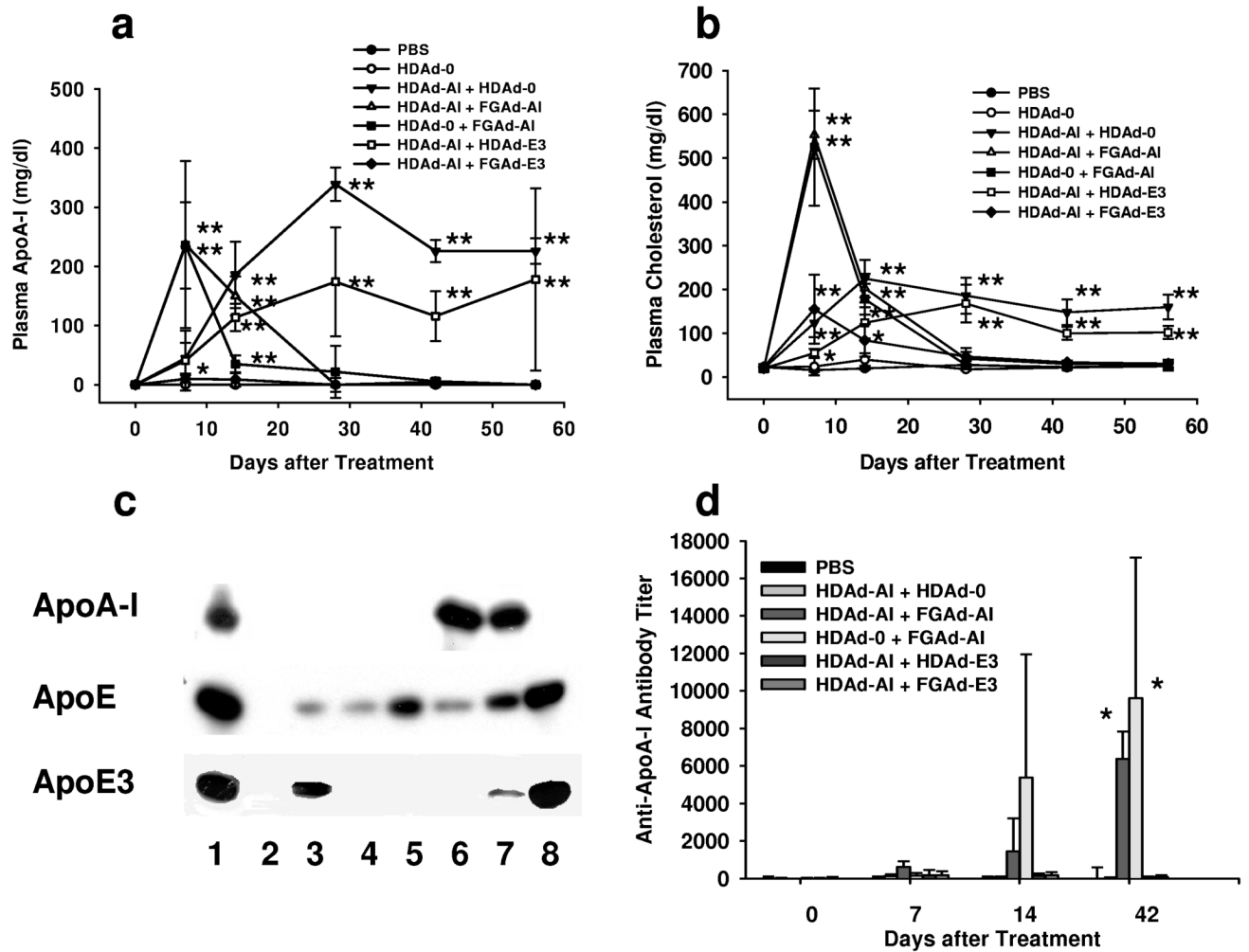


Figure 5.

Co-injection of FGAd vectors suppresses hAPOA1 expression mediated by HDAd-AI vector. (a) Plasma human APOA1 levels in APOA1^{-/-} mice treated with Ad vectors. *p<0.05 vs. PBS, **p<0.01. (b) Plasma cholesterol levels in APOA1^{-/-} mice after intravenous injection of Ad vectors. *p<0.05 vs. PBS, **p<0.01. (c) Immunoblot analysis of transgene expression. 0.1 μl of plasma collected from mice 8 weeks after treatment with various Ad vectors was separated by SDS-PAGE, and the presence of transgene products was detected by immunoblot. Upper panel: goat anti-human APOA1 antibody which does not cross react with mouse APOA1; middle panel: goat anti-apoE antibody; lower panel: mouse monoclonal antibody against human APOE3. Lane 1: Human plasma; lane 2: APOE^{-/-} mouse; lane 3: APOE^{-/-} mouse treated with HDAd-E3; lane 4: APOA1^{-/-} mouse treated with FGAd-AI + HDAd-0; lane 5: APOE^{-/-} mouse treated with HDAd-mouse APOE; lane 6: APOA1^{-/-} mouse treated with HDAd-AI + HDAd-0; lane 7: APOA1^{-/-} mouse treated with HDAd-AI and HDAd-E3; lane 8: APOA1^{-/-} mouse treated with HDAd-AI + FGAd-E3. (d) Generation of anti-hAPOA1 antibodies after intravenous co-injection of various Ad vectors. *p<0.05 (vs. day 0).

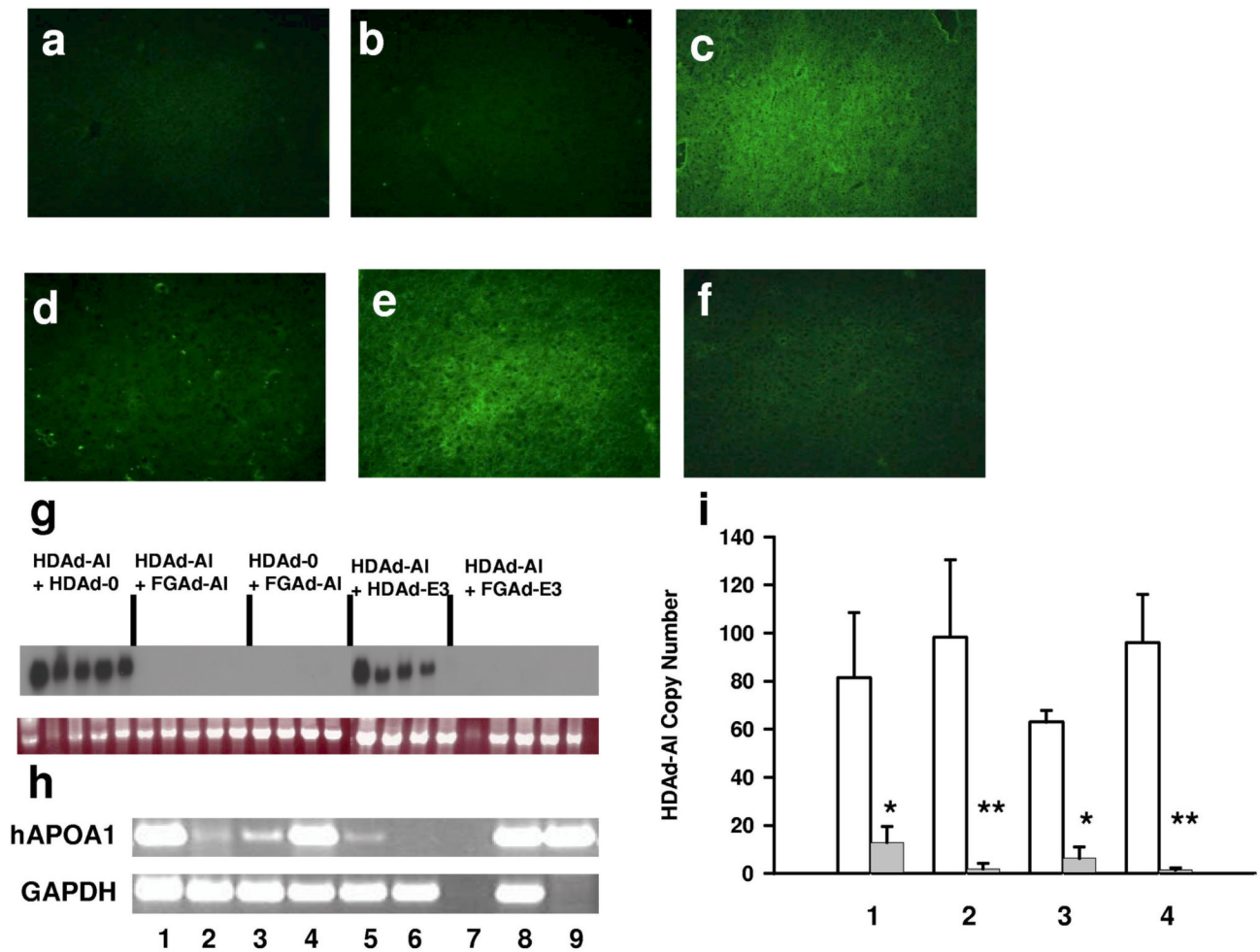


Figure 6.

Human APOA1 expression and HDAd vector copy number in liver of APOA1^{-/-} mice 56 days after treatment with various Ad vectors. Human APOA1 was detected by immunofluorescence. (a) PBS. (b) HDAd-0. (c) HDAd-AI + HDAd-0. (d) HDAd-AI + FGAd-AI. (e) HDAd-AI + HDAd-E3. (f) HDAd-AI + FGAd-E3. (g) Northern blot analysis. Top panel: APOA1 mRNA; bottom panel: 18S RNA. APOA1 mRNA was quantified by phosphorimager. The arbitrary APOA1 mRNA levels were $2,344 \pm 1,322$ (mean \pm SD, $n=4-5$) in HDAd-AI + HDAd-0, 0 ± 0 in HDAd-AI + FGAd-AI, 0 ± 0 in HDAd-0 + FGAd-AI, $1,875 \pm 1,294$ in HDAd-AI + HDAd-E3 and 5 ± 11 in HDAd-AI + FGAd-E3. (h) RT-PCR analysis. Total cellular RNA was extracted from the liver and PCR was performed after reverse transcriptase reaction using random hexamer. Top panel: hAPOA1 mRNA; bottom panel: GAPDH mRNA. 1: HDAd-AI + HDAd-0; 2: HDAd-AI + FGAd-AI; 3: HDAd-0 + FGAd-AI; 4: HDAd-AI + HDAd-E3; 5: HDAd-AI + FGAd-E3; 6: PBS; 7: PBS without reverse transcription; 8: human hepatoma cell line HepG2; 9: 5 ng of human APOA1 cDNA clone in KS. (i) Vector copy number. HDAd copy number was determined by Q-PCR and expressed as mean \pm SD copies/haploid genome. Open bar: vector copy number at day 1; closed bar: vector copy number at day 56. 1: HDAd-AI + HDAd-0 (81.5 ± 27.1 at day 1, 12.9 ± 6.7 at day 56); 2: HDAd-AI + FGAd-AI (98.3 ± 32.1 , 1.9 ± 2.3); 3: HDAd-AI + HDAd-E3 (63.0 ± 4.9 , 6.3 ± 4.8); 4: HDAd-AI + FGAd-E3 (96.1 ± 20.0 , 1.4 ± 0.9). * $p < 0.01$ ($n=4-5$, vs. baseline), ** $p < 0.01$ [$n=4-5$], vs. baseline, but

p<0.05 vs. copy number in mice treated with HDAd-AI + HDAd-0 at day 56]. The HDAd-AI vector was not detected in PBS control group.

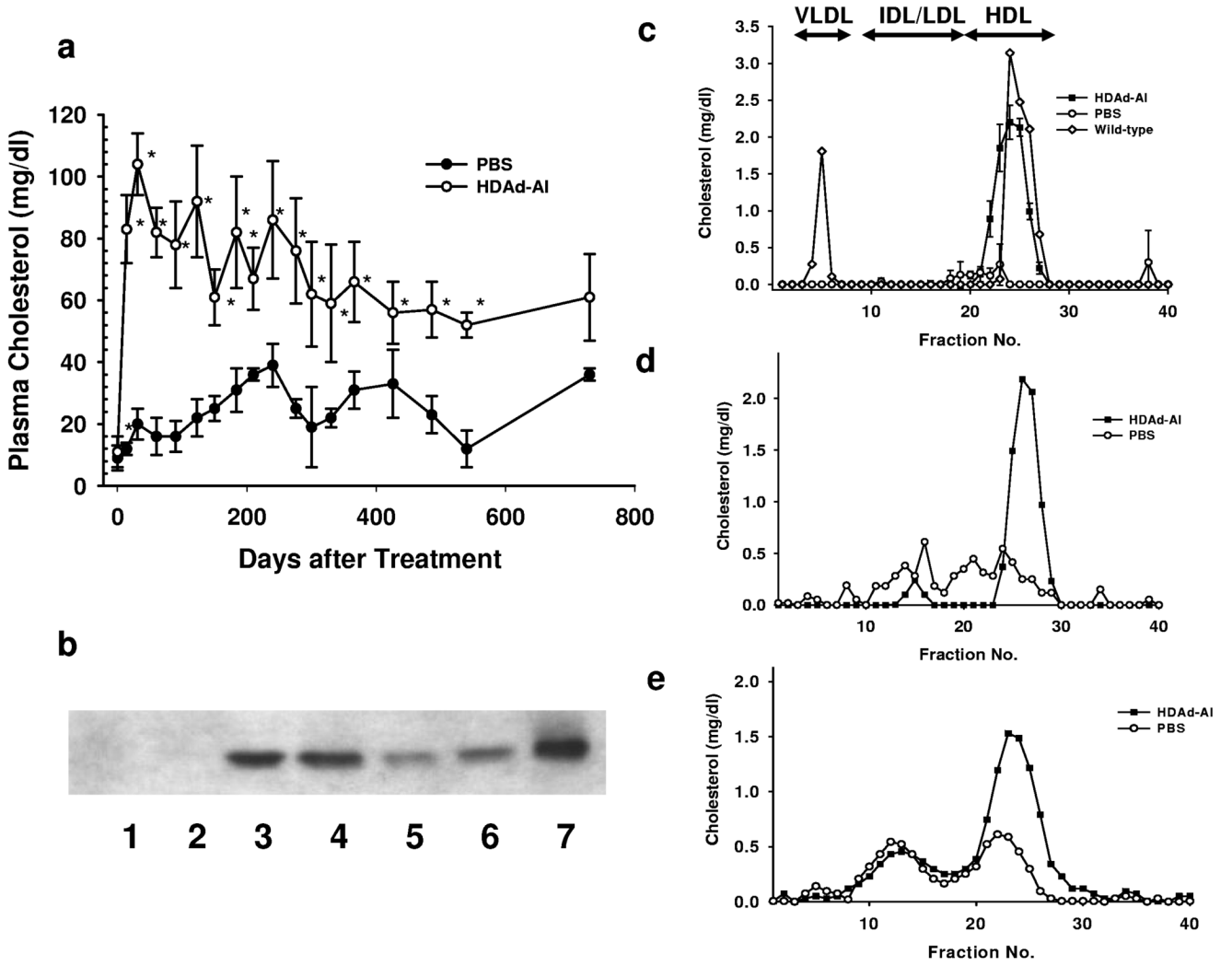


Figure 7. Long-term correction of hypoalphalipoproteinemia in APOA1^{-/-} mice by a single injection of HDAd-AI. (a) Plasma cholesterol levels. *p<0.01 (vs. PBS). (b) Immunoblot analysis of plasma collected 730 days after the treatment. Lanes 1 and 2: PBS; Lanes 3-6: HDAd-AI. Lane 7: human plasma (positive control). (c-e) FPLC profile. Plasma was collected from the mice 366 (c), 540 (d) and 730 (e) days after a single injection of HDAd-AI (4.5×10^{12} VP/kg), or PBS. In (c), lipoprotein profile of wild type C57BL/6 mice is shown.

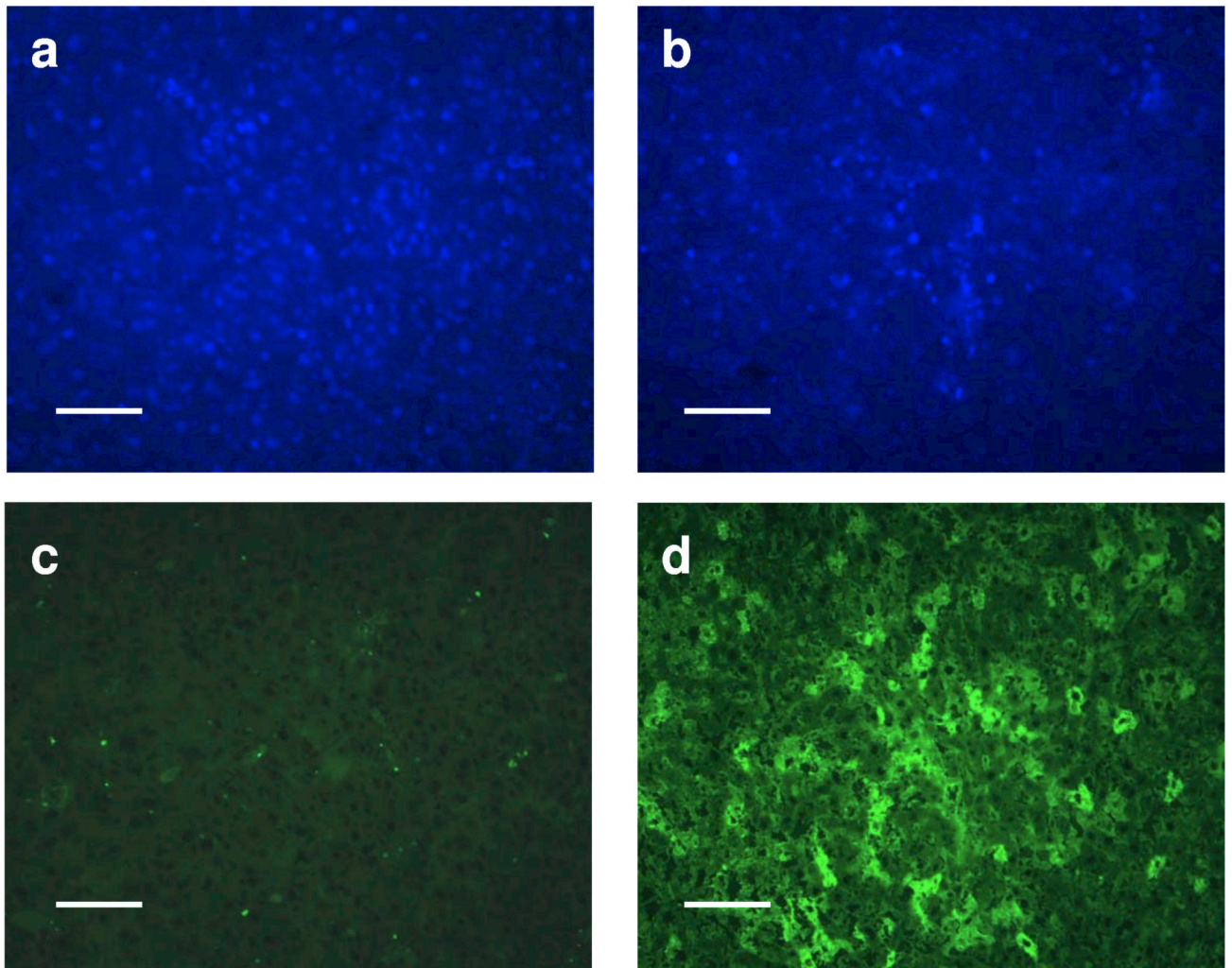


Figure 8. Immunofluorescence of liver sections of APOA1^{-/-} mice 730 days after treatment with HDAd-AI (4.5×10^{12} VP/kg) or PBS. Upper panel: DAPI staining; lower panel: detection of APOA1 immunoreactivity using an FITC-labeled rabbit anti-goat IgG. Left panel: PBS; right panel: HDAd-AI. The bar shows 100 μ m.

Table 1

Liver pathology		Day 3	Day 8	Day 15	Day 80
Baseline					
Normal or small foci of lobular hepatitis: 5-6 mononuclear cells	PBS	Rare tiny foci of inflammation or necroinflammation with PMN's and lymphocytes	Rare to few foci of necroinflammation	Multiple small foci of necroinflammation or one small focus of hepatitis, 1 + microsteatosis	Multiple small foci of necroinflammation or a few foci of hepatitis
	HDAd-AI	0 – 1 + microsteatosis, slight decrease in glycogen	Rare to few foci of inflammation or necroinflammation	Many tiny foci of inflammation or a few foci of lobular hepatitis, decreased glycogen	A few tiny or small foci of hepatitis
	FGAd-AI	Increased mitoses, slight lymphocyte adherence to endothelium, rare foci of necroinflammation, 1 + microsteatosis	4 + diffuse necrosis, inflammation, and hepatocellular atypia. Increased mitoses	4 + severe diffuse hepatocellular variation and atypia, degeneration necrosis, increased mitoses, rare or moderate inflammation	2 + necroinflammation and hepatocellular variation or atypia, or 1 + variation in hepatocellular nuclei with anisocytosis, rare foci of inflammation

APOA1^{-/-} mice were treated with 4.5×10^{12} VP/kg of HDAd-AI, FGAd-AI or PBS. The histopathological analysis was performed by a pathologist (M.F.) who was blinded to the type of treatment that the mice had received.

Table 2

Structures of adenoviral vectors used for co-injection

Vector	Backbone	Promoter	Gene	PolyA signal
HDAAd-AI	Stuffer DNA	Human APOA1 gene	APOA1 gene	APOA1 gene polyA
HDAAd-0	Stuffer DNA + 0.4kb Ad5 right end containing the E4 promoter	none	none	none
HDAAd-E3	Stuffer DNA	Human APOE3 gene + 1.7kb APOE3 gene liver control region	APOE3 gene	APOE3 gene polyA
FGAd-AI	E1 deleted Ad5 genome	CMV	APOA1 cDNA	SV40 polyA
FGAd-E3	E1 deleted Ad5 genome	CMV	APOE3 cDNA	SV40 polyA
FGAd-VLDLR	E1 deleted Ad5 genome	CMV	VLDLR cDNA	SV40 polyA